33rd Annual International Conference of the IEEE EMBS
Boston, Massachusetts USA, August 30 - September 3, 2011

Information transfer between neurons in the motor cortex triggered by visual cues

Sanggyun Kim, Kazutaka Takahashi, Nicholas G. Hatsopoulos, and Todd P. Coleman

Abstract— **It was previously shown that beta oscillations of local field potentials in the arm area of the primary motor cortex (MI) of nonhuman primates propagate as travelling waves across MI of monkeys during movement preparation and execution and are believed to subserve cortical information transfer. To investigate the information transfer and its change over time at the single-cell level, we analyzed simultaneously recorded multiple MI neural spike trains of a monkey using a Granger causality measure for point process models before and after visual cues instructing the onset of reaching movements. In this analysis, we found that more pairs of neurons showed information transfer between them after appearances of upcoming movement targets than before, and the directions of the information transfer across neurons in MI were coincident with the directions of the propagating waves. These results suggest that the neuron pairs identified in the current study are the candidates of neurons that travel with spatiotemporal dynamics of beta oscillations in the MI.**

I. Introduction

BETA oscillations in local field potential (LFP) observed across the arm area of the primary motor cortex (MI) of nonhuman primates propagate as plane waves along the rostrocaudal axis of the motor cortex during motor preparation and execution, and are believed to subserve cortical information transfer [1]. They represent the summed activity of multiple postsynaptic potentials near the recording electrode site; however, little is known about the relationship between the wave propagation of cortical oscillations and the information flow among individual neurons across the motor cortex. Recently, directed information between pairs of neurons was studied using multiple spike trains in the MI of a monkey [2], but they considered only pairwise directed information and did not analyze how the network might change in relationship to the stimulus.

In this paper, by simultaneously recording the ensemble neural spiking activity across the arm area of the MI cortex, we investigate information transfer between neurons and the network change before and after visual cues instructing the reaching movement. Recently methods that attempt to identify associations between neurons were developed [3], [4], but they provided little insight into the directional information transfer between them. The statistical measure of causality that has primarily been used to assess information transfer in the neuroscience community [5], [6] comes from Granger's notion of causality in the economics literature [7]: if past values of y contain information that helps predict x above and beyond the information contained in past values of x alone, then y is said to Granger-cause x. Its mathematical formulation is based on the multivariate autoregressive (MVAR) modeling of processes.

However, it is difficult to apply this method directly to spike train data due to its binary nature. To address this issue, in the current study we used a point process framework for assessing directional interactions between neurons in [8] to test how a network of neurons exhibiting causal interactions changes around the onset times of visual stimuli instructing the upcoming reaching movement. Previous studies [1], [9] have shown that, regardless of slight changes in behavioral tasks, beta oscillation waves often emerge after presentation of visual cues. Thus by looking at state changes of neurons around the time of the visual stimuli we could get more insight as to what class of neurons were participating in beta oscillation wave propagation and how those neurons were connected.

The rest of this paper is organized as follows. Section II describes behavioral tasks and data collection and explains a point process framework for assessing the causal interactions between multiple neurons. Section III describes the analysis of neural data recorded in the motor cortex of a monkey, and Section IV discusses the analysis results.

II. Method

A. Behavior task and data collection

All of the surgical and behavioral procedures were approved by the University of Chicago IACUC and conform to the principles outlines in the Guide for the Care and Use of Laboratory Animals. One monkey was trained to perform a visuomotor task using a two-link exoskeleton manipulandum [10]. The monkey was required to move a cursor on a horizontal screen that was aligned to the monkey's hand to the position of a target. When the monkey successfully reached the current target, a new target was displayed at a random location within a workspace while the current target disappeared. The monkey received a juice reward after successfully acquiring five or seven consecutive targets.

We recorded multiple single unit spiking activities from MI in a monkey using an Utah microelectrode array (Blackrock Microsystems; 1 mm in length and 400μm interelectrode spacing) implanted contralateral to the moving

S. Kim and T.P. Coleman are with Department of Electrical and Computer Engineering, University of Illinois at Urbana-Champaign, 1308 W. Main Urbana, IL 61801 USA. {sgkim1, colemant}@illinois.edu. This work was supported by NSF STC Grant CCF-0939370, MuSyC through the FCRP Program, and the AFOSR Complex Networks Program via Award FA9550-08-1-0079.

K. Takahashi and N.G. Hatsopoulos are with Department of Organismal Biology and Anatomy, University of Chicago, Chicago, IL 60637 USA. {kazutaka,nicho}@uchicago.edu. This work was supported by NIH 2R01 NS045853-05.

arm. Neural spikes from up to 96 channels were recorded at 30 kHz. Spike waveforms were sorted offline using a semiautomated method incorporating a previously published algorithm [11]. Signal to noise ratio (SNR) for each unit were defined as the difference in mean peak to trough voltage divided by twice the mean standard deviation computed from all the spikes at each sample points. All the units with SNR<3 were discarded for the current study. The data for each neuron was converted to a binary time series with 1 ms time resolution. Among 115 neurons available for analysis, we used only 25 neurons that were recorded from electrodes located on even numbered rows and columns on 10 x 10 grid on the multielectrode array due to the computational load. Three data sets, each with 1,000 consecutive successful trials, were constructed. Each data set consisted of three sub data sets collected from the following time windows in relation to visual cue onset, $[-100, 50]$, $[50, 200]$, and $[200, 350]$ ms.

B. Analysis

The discrete, all-or-nothing nature of a sequence of neural spike train together with their stochastic structure suggests that neural spike trains may be regarded as point processes [12], [13]. A neural point process model is completely characterized by its conditional intensity function (CIF), $\lambda(t|H(t))$, where $H(t)$ denotes the spiking history of all neurons in the ensemble up to time t. In this work, $H(t)$ is defined in the interval $[t-MW, t)$, which is divided into M non-overlapping rectangular windows of duration W; We denote the spike count of neuron n in a time window of length W covering the time interval $[t-mW, t-(m-1)W)$ as $R_{n,m}(t)$ for $n = 1, ..., N$ and $m = 1, ..., M$. In this analysis we intuitively set M to 5 and W to 3 ms to obtain a relatively small number of parameters while maintaining the temporal resolution. The CIF, $\lambda(t|H(t))$, represents the firing rate of a neuron at time t, thus the probability that a neuron will fire a single spike in a small interval $[t, t+\Delta)$ can be approximated as $\lambda(t|H(t))\Delta$. In the generalized linear model (GLM) framework, we modeled the log CIF as a linear combination of the covariates, $H(t)$, which describe the neural activity dependencies [14]. Thus the logarithm of the CIF for neuron i is expressed by

$$\log \lambda_i(t|\boldsymbol{\theta}_i, H_i(t)) = \theta_{i,0} + \sum_{n=1}^{N}\sum_{m=1}^{M} \theta_{i,n,m} R_{n,m}(t) \qquad (1)$$

where $\theta_{i,0}$ relates to a background level of activity, and $\theta_{i,n,m}$ represents the effect of ensemble spiking history $R_{n,m}(t)$ of neuron n on the firing probability of neuron i at time t for $n = 1, ..., N$ neurons.

Recently a point process framework for assessing causal relationship between neurons was proposed in [8]. Based on Granger's definition on the causality [7], a potential causal relationship from neuron j to i can be assessed based on the log-likelihood ratio given by

$$\log \frac{\Pr(\text{future of } i|\text{past of } i, \text{past of } j)}{\Pr(\text{future of } i|\text{past of } i)}. \qquad (2)$$

If past values of neuron j contain information that helps predict future value of neuron i beyond the information contained in past values of neuron i alone, $\Pr(\text{future of } i|\text{past of } i, \text{past of } j)$ is greater than $\Pr(\text{future of } i|\text{past of } i)$, thus the log likelihood ratio of (3) is always greater than or equal to zero. The equality holds when neuron j has no causal influence on i. This statistical framework for assessing Gragner causality can be applied to any modality as well as binary neural spike train data [15]. However, the pairwise causality measures based on (3) may give us a misleading picture of the relationships between neurons if the detected associations are caused by common inputs or mediated by other neurons [16]. This pairwise Granger causality concept can be extended to a general framework for identifying the causal relationships between multiple neurons [8], [17] based on

$$\log \frac{\Pr(\text{future of } i|\text{past of everyone})}{\Pr(\text{future of } i|\text{past of everyone except } j)}. \qquad (3)$$

Thus, the Granger causality from neuron j to i is identified in the following. First, the point process likelihood function of neuron i, denoted by $L_i(\boldsymbol{\theta}_i|H(t))$, is calculated using the parametric CIF of (1); It relates the ith neuron's spiking probability to possible covariates such as its own spiking history as well as the concurrent activity of other simultaneously recorded neurons [14]. Next, we assess the causal relationship from neuron j to i by calculating the relative reduction in the likelihood of neuron i obtained by excluding the covariates effect of neuron j (spiking history of neuron j) compared to the likelihood obtained using all the covariates (spiking history of all neurons). The log-likelihood ratio, Γ_{ij}, is given by

$$\Gamma_{ij} = \log \frac{L_i(\boldsymbol{\theta}_i)}{L_i(\boldsymbol{\theta}_i^j)} \qquad (4)$$

where the parameter vector $\boldsymbol{\theta}_i^j$ is obtained by re-optimizing the parametric likelihood model after excluding the effect of neuron j. Since the likelihood $L_i(\boldsymbol{\theta}_i)$ is always greater than or equal to the likelihood $L_i(\boldsymbol{\theta}_i^j)$, the log-likelihood ratio Γ_{ij} is always greater than or equal to 0. If the spiking activity of neuron j has a causal influence on that of neuron i in the Granger sense, the likelihood $L_i(\boldsymbol{\theta}_i)$ is greater than $L_i(\boldsymbol{\theta}_i^j)$. The equality holds when neuron j has no influence on i. The Granger causality measure given by (4) provides an indication of the extent to which the spiking history of neuron j affects the spike train data of neuron i. Thus we can construct an $N \times N$ Granger causality matrix, whose (i, j)th element represents the extent to which neuron j has a causal influence on neuron i for $i, j = 1, ..., N$ neurons. This $N \times N$ matrix enables us to draw the causality neural network graph with N nodes (neurons) connected by directed edges representing the relative strength of causal effects. This causality network represented the relative strength of estimated causal interactions between neurons; however, it provided little insight into which of these interactions are

statistically significant. To address this issue, a multiple hypothesis testing was performed based on the likelihood ratio test statistic since we can show that 2 times log-likelihood ratio given by (4) asymptotically follows χ^2_M where M is equal to the difference in dimensionality of the two models [18], [19]. Thus, another $N \times N$ causal connectivity matrix was constructed, whose (i, j)th element corresponds to either statistically significant or insignificant interaction.

Once the causality matrix was obtained for each sub data set, degrees for each neuron that showed any statistically significant interactions were computed across all three sub data sets for all three data sets. The degree for neuron i is defined as the number of neurons that are coupled to i by at least one interaction [20]. Then degrees of all neurons per sub data set was obtained for all nine sub data sets to show consistency of causality networks across three data sets at same time windows. Another measure of network consistency across data sets was obtained simply by counting the number of pairs exhibiting causal interactions.

III. Results

The causality networks between the recorded neural spike trains were identified using the method in [8], and the results were illustrated in Fig. 1. Fig. 1 (a), (b), and (c) show the statistically significant causal interactions at different timings in relation to the visual cue onset: Time Window 1 for $[-100, 50]$ ms, 2 for $[50, 200]$ ms, and 3 for $[200, 350]$ ms, respectively. The relative positions of neurons in the diagrams correspond to the relative positions of the electrode on the array where the neurons were detected. Adjacent neurons (nodes) were recorded from a same electrode. The location of the array is such that the lower right corner is oriented caudal and the upper left rostral.

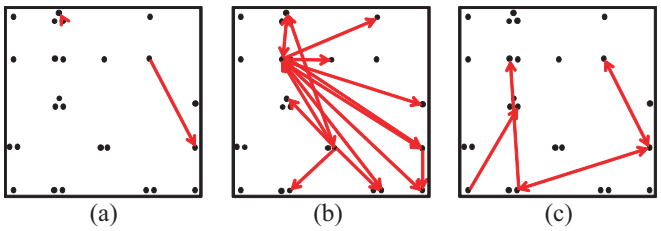

Fig. 1. A diagram of causality networks estimated at different timings in relation to the visual cue onset: Time Window 1 for $[-100, 50]$ ms, 2 for $[50, 200]$ ms, and 3 for $[200, 350]$ ms, respectively. (a) Causality network estimated for Time Window 1 is illustrated. (b) Causality network estimated for Time Window 2 is illustrated. More neurons were causally influencing each other. (c) Causality network estimated for Time Window 3 is illustrated. Less significant causal interactions were detected than Time Window 2.

As shown in Fig. 1, most causal interactions were detected for Time Window 2 than other two intervals. These causality networks were obtained from the data set1, and we obtained similar results using data sets 2 and 3 as well. In order to look into the causality network consistency over data sets, we plotted the degrees of all neurons for 3 data sets in Fig. 2. All data sets had similar distributions of degrees and same 'hub' neurons 9 and 15 - neurons with unusually high degree. Interestingly neurons recorded from a same electrode were not interacting with one another, but they were causally influencing on neurons from different electrodes.

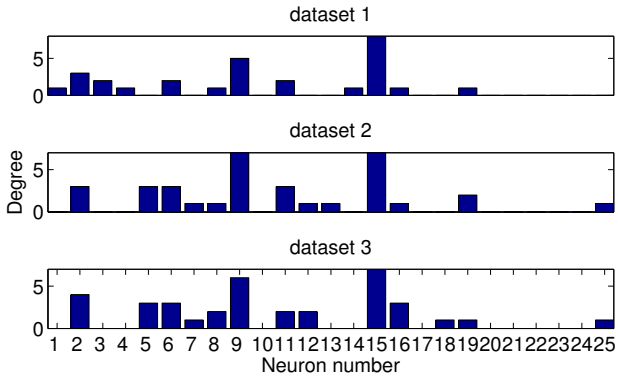

Fig. 2. The degrees of all neurons obtained for Time Window 2 are illustrated over 3 data sets. Similar distributions of degrees and same hub neurons 9 and 15 were observed for all 3 data sets.

Fig. 3 shows that across three different data sets, the numbers of pairs exhibiting statistically significant causal relationships are highest over a time window 2 of $[50, 200]$ ms after the visual cues instructing the locations of the upcoming movements.

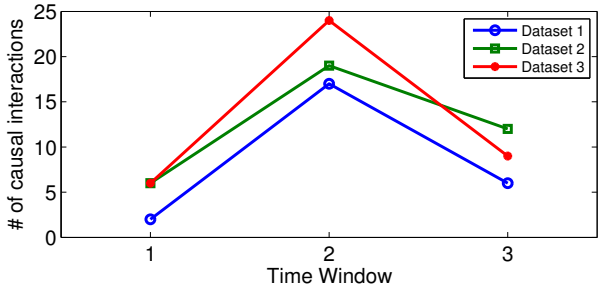

Fig. 3. Number of statistically significant causal interactions at different timings in relation to the visual cue onset. Each data set showed the maximum number of causal relations right after visual cue presentations, Time Window 2.

IV. Discussions

Beta oscillations in the MI during motor preparation propagate as waves across the surface of the motor cortex along dominant spatial axes characteristic of the local circuitry of the motor cortex [1]. In order to investigate whether we can observe the same information transfer between neurons, the Granger causality measure for point process models [8] was applied to multiple spike train data recorded in the MI. As shown in Fig. 1, more causal interactions were detected around visual cues, and the direction of causal interactions was roughly aligned with simultaneously recorded beta oscillations propagating wave direction [1] and a group of neurons that exhibited significant power in frequency range of beta oscillations in their spike rates around cue appearances [9].

We verified that these results were consistently observed over 3 data sets. Also, as Fig. 3 illustrates, the maximum numbers of neuron pairs show statistically significant causal relationships over $[50, 200]$ ms after appearance of visual cues around which phase of beta oscillations is locked and evoked beta traveling waves emerge [9].

Thus it is plausible that the neuron pairs identified in the current study are the candidates of neurons that travel with planar waves of beta oscillations in MI.

V. ACKNOWLEDGMENTS

We would like to thank Jacob Reimer who collected the behavioral and neural data used for the current work.

REFERENCES

[1] D. Rubino, K. A. Robbins, and N. G. Hatsopoulos, "Propagating waves mediate information transfer in the motor cortex," *Nat Neurosci*, vol. 9, no. 12, pp. 1549–1557, 2006.

[2] C. Quinn, T. P. Coleman, N. Kiyavash, and N. G. Hatsopoulos, "Estimating the directed information to infer causal relationships in ensemble neural spike train recordings," *Journal of Computational Neuroscience*, vol. 30, pp. 17–44, 2011.

[3] C. D. Brody, "Correlations without synchrony," *Neural Comput*, vol. 11, pp. 1537–1551, 1999.

[4] G. L. Gerstein and D. H. Perkel, "Simultaneously recorded trains of action potentials: analysis and functional interpretation," *Science*, vol. 164, pp. 828–830, 1969.

[5] A. Roebroeck, E. Formisano, and R. Goebel, "Mapping directed influence over the brain using Granger causality and fMRI," *Neuroimage*, vol. 25, pp. 230–242, 2005.

[6] A. Brovelli, M. Ding, A. Ledberg, Y. Chen, R. Nakamura, and S. L. Bressler, "Beta oscillations in a large-scale sensorimotor cortical network: directional influences revealed by Granger causality," *Proc. Natl. Acad. Sci. USA*, vol. 101, pp. 9849–9854, 2004.

[7] C. Granger, "Investigating causal relations by econometric models and cross-spectral methods," *Econometrica*, vol. 37, pp. 424–438, 1969.

[8] S. Kim, D. Putrino, S. Ghosh, and E. N. Brown, "A granger causality measure for point process models of ensemble neural spiking activity," *PLoS Comput Biol*, vol. 7, no. 3, p. e1001110, 03 2011.

[9] K. Takahashi and N. Hatsopoulos, "Copropagating waves of local field potentials and single-unit spiking in motor cortex." Socity for Neuroscience, Nov 2007.

[10] S. Scott, "Apparatus for measuring and perturbing shoulder and elbow joint positions and torques during reaching," *Journal of Neuroscience Methods*, vol. 89, no. 2, pp. 119 – 127, 1999.

[11] C. Vargas-Irwin and J. Donoghue, "Automated spike sorting using density grid contour clustering and subtractive waveform decomposition," *Journal of Neuroscience Methods*, vol. 164, no. 1, pp. 1 – 18, 2007.

[12] D. Daley and D. Vere-Jones, *An Introduction to the Theory of Point Process*. Springer-Verlag, New York, 2003.

[13] E. N. Brown, R. Barbieri, U. T. Eden, and L. M. Frank, *Computational Neuroscience: A Comprehensive Approach*. CRC, 2003, vol. 649, ch. Likelihood methods for neural spike train data analysis, pp. 253–286.

[14] W. Truccolo, U. T. Eden, M. R. Fellows, J. P. Donoghue, and E. N. Brown, "A point process framework for relating neural spiking activity to spiking history, neural ensemble, and extrinsic covariate effects," *Journal of Neurophysiology*, vol. 93, no. 2, pp. 1074–1089, 2005.

[15] S. Kim and E. N. Brown, "A general statistical framework for assessing Granger causality," *IEEE ICASSP 2010*, pp. 2222–2225, Mar. 2010.

[16] Y. Chen, S. L. Bressler, and M. Ding, "Frequency decomposition of conditional granger causality and application to multivariate neural field potential data," *Journal of Neuroscience Methods*, vol. 150, no. 2, pp. 228–237, 2006.

[17] C. Quinn, N. Kiyavash, and T. P. Coleman, "Equivalence between minimal generative model graphs and directed information graphs." to appear, IEEE International Symposium on Information Theory, Jul 2011.

[18] A. Dobson, *An introduction to generalized linear model*. CRC Press, 2002.

[19] Y. Pawitan, *In all likelihood: statistical modeling and inference using likelihood*. Oxford University Press, New York, 2001.

[20] M. E. J. Newman, *Networks: An introduction*. Oxford University Press, New York, 2010.